Laser spark ignition of a jet diffusion flame

Tran X. Phuoc*, C.M. White, D.H. McNeill[1]

US Department of Energy, National Energy Technology Laboratory, MS 84-340, P.O. Box 10940, Pittsburgh, PA 15236, USA

Received 24 August 2001; accepted 19 November 2001

Abstract

In this work we report preliminary results on the laser ignition of a jet diffusion flame with jet flow rates ranging from 35 ($Re = 1086$) to 103 cm^3/s ($Re = 3197$). The laser spark energy of about 4 mJ was used for all the tests. The relative amounts of fuel and air concentrations at the laser focus have been estimated using a variant of laser-induced breakdown spectroscopy. The ignition and the flame blow out times were measured using the time-resolved OH emission. Ignition times in the range from 3 to about 10 ms were observed depending on the experimental conditions and they increased towards the rich as well as the lean sides. The early time and late-time OH emissions indicate that chemical reactions during the initial stage of the blast wave expansion are not immediately responsible for the ignition. The ultimate fate of an ignition depends on the reactions at later times which determines whether the gas could undergo a transition from hot plasma to a propagating flame.

1. Introduction

When a laser beam with an irradiance $\geqslant 10^{10}$ W/cm^2 interacts with a gas, the gas breaks down owing to multiphoton ionization or electron avalanche [1–7]. This laser-induced gas breakdown process can be used to ignite gaseous combustible mixtures [8–17] and liquid fuel sprays [18], or even to extinguish a diffusion flame [9]. Compared with other laser ignition types, such as laser-induced thermal ignition, or laser-induced photochemical ignition, this type of laser ignition does not require a close match between the laser wavelength and the target molecule's absorption

wavelength to create a spark. Although the laser wavelength does influence the threshold for breakdown, once breakdown is achieved, ignition depends primarily on the amount of energy absorbed in the plasma. Laser ignition offers many advantages over comparing with other conventional ignition methods such as electric spark plugs, plasma jet igniters, or rail plugs. With laser ignition, the ignition location and timing, as well as the ignition energy and deposition rate can be controlled easily. Laser ignition is non-intrusive, so that heterogeneous effects and wall heat loss can be eliminated. And, above all, laser ignition is capable of providing center-ignition and/or multiple-ignition sites that can be programmed to ignite a combustible mixture either sequentially or simultaneously. These advantages are potentially important for fuel-lean combustion and high-speed combustion applications. The benefits of multi-point laser ignition have been discussed by Ronney [19] and demonstrated experimentally by Phuoc [20] and Morsy et al. [21].

In a study on the effects of the ignition locations and the multi-point ignition on the combustion times and pressures for a stoichiometric methane–air mixture, Phuoc [20] found that two-point ignition always yielded higher pressure and shorter combustion times than single-point ignition. The effect of two-point ignition was most evident in the fuel-lean and fuel-rich regions and less so in the near-stoichiometric region. With center-ignition, the flame had a nearly spherical shape and the combustion time was about 30% shorter than that with wall-ignition. When flames were created by two-point ignition, they rapidly stretched in the vertical direction as the flame fronts approached together. The region between the two flames was preheated and compressed. This might increase the combustion rate. The time required for complete combustion was 50% shorter than that required for the wall-ignition case, and about 25% shorter than the center-ignition case.

Morsy et al. [21] studied two-point ignition using a different approach. The laser beam was focused using a f200 mm lens to create spark ignition at a desired location and the transmitted laser energy was directed into a conical cavity in an aluminum plate for cavity ignition. In comparison with single-spark or single-cavity ignition, they found that the reduction in the flame initiation time by the two-point spark/cavity ignition was about 45–69% and it became more pronounced at lower initial combustion chamber pressures. The total combustion time for the two-point ignition case was also reduced by about 28–45% depending on the initial pressure. They also reported that the center of the combustion chamber is the optimum spark position for reducing both the flame initiation time and the combustion time.

In the present work, we study the laser ignition of a methane diffusion jet flame. Although there are many difficulties owing to the complexity of the jet geometry, the dynamic interaction between the spark and the flow, etc., we have been able to investigate the effectiveness of the laser ignition in a turbulent flow environment. In addition, this study also provides the opportunity to demonstrate the benefits associated with the non-intrusiveness and the movability of the ignition location which are characteristics of the laser ignition. When a fuel jet emerges into quiescent air, the jet expands and air entrains the jet. The entrained air mixes with the fuel to create combustible mixtures with different fuel and air concentrations across the flow field. Since the dominance of any particular process including mixing at a particular

distance depends on flow parameters such as the jet velocity, the jet diameter, the air entrainment, etc., the location of the optimum fuel-to-air ratio for successful ignition will change when the flow condition changes. Thus, efficient ignition of a variable jet flow requires the ignition location to be changeable. Using conventional ignition techniques such as electric spark plugs for this application is too complex and more difficult. With laser ignition, however, a spark volume can be created at any location along the jet vertical axis or across the jet in the radial direction by simply using an optical scanning device. Thus, use of the laser ignition for this application is more favorable.

The present measurements will be made of the ignition probability, the distributions of the ignition and the flame blow out times, the relative fuel and air concentrations, and the time-resolved OH emission. A rough estimate of the equivalence ratio to support the distribution of the ignition probability will also be carried out. These results are presented in the following sections. A discussion on the roles of the early time and the late-time chemical reactions in the laser ignition process will also be given.

2. Experimental apparatus

The experimental apparatus used in this study has been described elsewhere [6,7]. The gas jet was produced using a contoured stainless steel nozzle with an inlet diameter of 2.5 cm and a flat exit tip diameter of 0.15 cm. The nozzle was mounted on a three-axis translation stage and was aimed vertically upward into the laboratory air. Research grade methane (99.99%, density $\rho = 0.652\,\mathrm{kg/m^3}$, and viscosity $\mu = 1.40 \times 10^{-5}\,\mathrm{kg/m\,s}$) from a high-pressure cylinder was fed to the nozzle using a gas handling system. The gas handling system was controlled by a Program Logic Controller (PLC), via an air-actuated gas control box, and was interlocked with appropriate sensors to monitor the vent exhaust and gas leak. The pressure was regulated and set at 160 kPa throughout the tests.

Sparks were produced using a single-mode, Q-switched Nd-YAG laser (Quantel, Brilliant W). The laser produced a 0.6-cm-diameter beam at a wavelength of 1064 nm with a 5.5 ns pulse duration. The beam was focused into the gas jet by a 100 mm focal length lens after passing through a 1–99% variable beam splitter. With this laser system, the focal spot diameter and length are estimated to be 22.5 and 345 μm, respectively. In order to have a well controlled beam energy throughout the experiments, the laser parameters were held constant, while the delivered laser energy was varied by rotating the beam splitter about its center. The pulse energy was measured using two pyroelectric energy meters (Oriel 70713), together with two energy readout units (Oriel 70833). One detector was placed on the side of the fuel injection nozzle, opposite the incoming laser beam to measure the transmitted laser energy and the other was placed behind the variable beam splitter which was located in front of the lens to measure the input laser energy. To preserve the quality of the laser beam throughout the experiments, the focal point was kept at a fixed location and the relative location of the laser spark along the jet axis was varied by translating

the gas nozzle vertically. Once a vertical location was chosen, the nozzle could be translated horizontally in a direction perpendicular to both the jet axis and the laser beam. The combined motions permit a complete radial and axial scan of the jet region.

The principal diagnostics are optical, along with a pyroelectric energy meter for measuring the incident and transmitted laser beam energies. Optical breakdown of the gas mixture by the laser pulse is generally detected by one or more photomultipliers combined with visible or near-ultraviolet bandpass filters to isolate particular emission wavelengths (e.g., of oxygen, hydrogen, or the OH radical). The signals from the detectors were fed into a fast Digital Phosphor Oscilloscope (Tektronix TDS35052). The response time of the unamplified photomultipliers is ~ 2 ns. (With an amplifier the response time is on the order of 20 μs.) Ignition and the development of the flame following ignition are also monitored with the aid of a long-wavelength visible and near-infrared photodetector, with a response time on the order of 10–100 μs. The detector response times are appropriate for the time intervals of interest: 5–500 ns for the laser-induced breakdown spark, 10–2000 μs for the interval between the spark and ignition of the gas, and 0.5–200 ms or more for the duration (blow out time) of the ignited flame.

3. Results and discussions

In this section we report and discuss our results on the laser ignition of a jet diffusion flame. In these experiments the jet flow rates ranging from 35 ($Re = 1086$) to 103 cm^3/s ($Re = 3197$) were used. The laser pulse energy, fluctuating between 15 and 15.5 mJ, was kept the same for all tests. The transmitted energy ranged from about 11 to 11.85 mJ. Thus, the laser energy absorbed in the spark was ~ 4 mJ, which is in the range of the ignition minimum reported by Phuoc and White [15].

3.1. Ignition probability

The ignition probability is defined as the ratio of the number of the successful ignition events divided by the total number of breakdown sparks. The ignition probability for a jet diffusion flame will depend strongly on the jet velocity and the location where the ignition source is applied. To determine the ignition probability we simply counted the number of ignition successes (or failures) out of 100 applied laser pulses. For the condition at which the flame is stable after it ignites, the counting was done using the single-firing mode. For the jet condition that the flame blow out after it ignites, the counting procedure is as follows: for each data set we used a total of 100 laser pulses that were fired continuously at 10 Hz. The onset of the laser pulse was monitored by a pyroelectric energy meter. The pulse energy is set high enough to ensure breakdown 100% of the time. The onset of both the laser-induced spark and the ignition event were monitored by the infrared detector. The signals from these detectors were fed into the digital oscilloscope which was triggered by the signal from the pyroelectric energy meter monitoring the laser pulse.

Typical oscilloscope traces of the signals representing the onset of the laser pulse, the breakdown spark and the ignition event are shown in Fig. 1. (Note that here the fall time for the pyroelectric signal (lower trace) is very long compared to the actual laser pulse duration.) It is clear that not all gas breakdown events lead to successful ignition. For example, the spark created by laser pulse A did not ignite the fuel jet while those produced by pulses B and C did.

This simple counting approach was used to determine the ignition probability for a diffusion jet flame at different locations in the jet and for different flow rates. The results are shown in Fig. 2

Fig. 2A shows the spatial distribution of the ignition probability for the fuel jet with a methane flow rate of 35 cm^3/s. Three locations along the jet axis were chosen so that the various mixing behaviors of the jet could be demonstrated. It was observed that when the flame is ignited by a spark at about 11 mm above the nozzle tip, the flame lifts away from the spark and becomes stable with its base situated steadily about 22 mm above the nozzle tip. The ignition probability was highest (50%) on the jet axis and fell off sharply at about 3 mm away from the axis. When sparks were created either 36 or 73.5 mm above the nozzle tip the flame propagated toward the nozzle tip and became stable. The ignition probability at 36 mm above the nozzle tip increased rapidly from about 10% near the jet axis to a maximum level of about 95% in the region around 4.5 mm off the jet axis. On moving further into the ambient air, the ignition probability decreases to about 65% at 6.2 mm off the jet axis. Further away from the nozzle tip, e.g., at 73.5 mm, the spatial distribution of

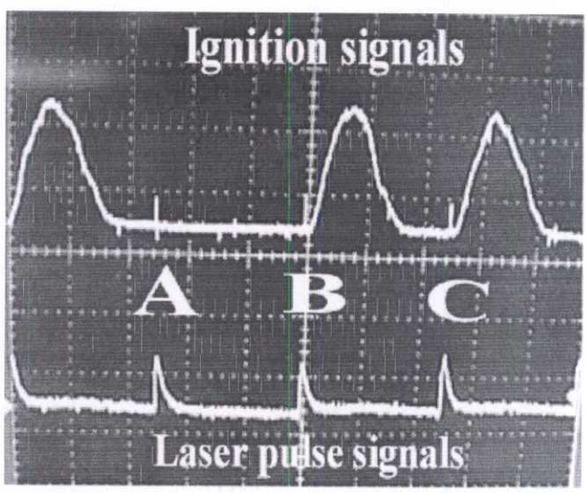

Fig. 1. Typical traces of the laser pulse monitor illustrating the use of the optical monitor for identifying whether ignition has taken place following laser breakdown. The horizontal axis corresponds to 100 ms/div. In the top trace the spark produced by signal A did not lead to ignition while those by signals B and C did.

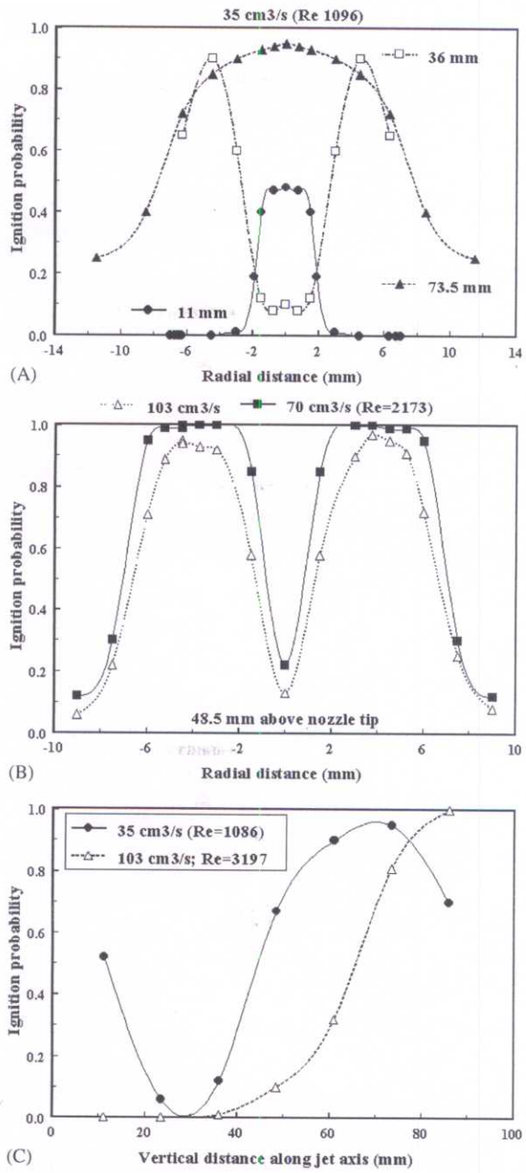

Fig. 2. Ignition probability profiles of the jet diffusion flame: (A) in the radial direction, effect of the vertical positions above the nozzle tip (flow rate: 35 cm^3/s; at 11, 36, and 73.5 mm); (B) in the radial direction, effect of the flow rate (48.5 mm above the nozzle tip, 70 and 103 cm^3/s); and (C) in the vertical direction on the jet axis, effect of the flow rates.

the ignition probability is quite different. The maximum 95% ignition probability is observed across the jet out to about 3 mm from its center. The ignition probability then decreases gradually, approaching 25% as far as 11.5 mm from the jet center.

Fig. 2B shows the effect of the flow rate on the distribution of the ignition probability across the jet at 48.5 mm from the nozzle tip. Flow rates of 70 ($Re = 2173$) and 103 cm^3/s ($Re = 3197$) were used. At these flow rates the flames were very unstable. When a spark was created in the region near the jet axis the flame was lifted to about 9 mm above the spark and then it was blown out to about 60–70 ms after ignition. When the flame was ignited in a low velocity region, such as near the jet boundary, the flame anchored to the spark with a weak stem and slanted slightly inward. The flame was then lifted away from the spark and blown out.

Fig. 2C shows the ignition probability along the jet axis for two flow rates. For a flow rate of 35 cm^3/s ($Re = 1086$) the ignition probability decreases from about 52% at 11 mm to about 4% at 23.5 mm, then it increased to about 95% at 73.5 mm, and finally fell off. For a flow rate of 103 cm^3/s ($Re = 3197$) the ignition probability increased along the jet axis and a 100% ignition probability was observed at 86 mm above the nozzle tip.

Experiments with higher pulse energies were also carried out but no significant effects of the pulse energy were observed. In fact as long as the pulse energy was sufficient to create 100% gas breakdown probability, any further increase in the pulse energy did not affect the observed distribution of the ignition probability. Thus, the distribution of the ignition probability reported in these figures can be attributed to the variations in the fuel-to-air ratio at various locations within the jet. Other factors such as turbulence intensity, velocity gradient at the ignition location also influence the ignition probability. In this present work, however, we will discuss only on the relationship between the ignition probability and the fuel-to-air ratio at the ignition location. It is known that when a fuel jet enters quiescent air, jet expansion and air entrainment occur. Entrained air mixes with the fuel to form a flammable mixture in the flow field. Since the mixing rate in this case depends on the turbulent interaction between the jet and the entrained air (which depends strongly on the jet velocity), the fuel and air concentrations across the jet and along its axis are different. In the region near the nozzle tip, entrained air does not have time to penetrate and mix with the fuel, so the fuel concentration across the jet might be too rich to ignite. Above the nozzle tip, since the air has sufficient time to penetrate into the jet, there is a region where the fuel concentration decreases from rich, to stoichiometric, to lean on moving radially toward the air side. As the latter site is further away from the nozzle tip, there is a flammable region where a stoichiometric fuel fraction exists across the jet. At the top of the jet, however, the flow field may become too lean to burn.

These features of the distribution of the fuel and air concentrations can be illustrated by using a variant of laser-induced breakdown spectroscopy. In essence, we examine the late time behavior of the laser spark in the fuel–air mixture. As reported by Phuoc and White [7], after a strong spectrally broad band background continuum (which is about 0.5 μs), most of the line radiation is at the wavelength of the OI triplet near 777 nm if the spark is created in air. If the spark is in methane the

strongest line radiation is at the wavelength of the H_α-line (656 nm), which is emitted by electronically excited hydrogen dissociated from the methane fuel. Thus, by examining the relative intensities of these lines from the spark in the fuel–air mixture one should be able to roughly estimate the fuel and air concentration of the mixture. We obtained the data using two PMTs. The PMTs were set up to view the spark using 1:1 imaging optics. One photomultiplier was used with a 1/8-m monochromator set to a 1.5 nm bandpass centered at 777 nm for monitoring the emission from the breakdown spark and the ensuing shocks by the OI triplet near 777 nm from atmospheric O_2. The other photomultiplier was used with a 10 nm bandwidth interference filter centered at ~656 nm for monitoring the analogous emission of the H_α-line (656.3 nm) from the methane fuel. The signals from the detectors were fed into the fast Digital Phosphor Oscilloscope (Tektronix TDS35052) which was triggered externally by a fast laser energy meter (Molectron, P5-01, the rise time of 500 ps). With the present optical setup, for the spark created in the stoichiometric methane–air mixture, the intensity of OI triplet varied between 14 and 15 mV and the intensity of the H_α-line was between 185 and 190 mV. Thus, the relative concentrations of methane and air with respect to their stoichiometric values and the equivalence ratios were deduced by normalizing the measured intensities of the OI triplet and the H_α-line by their stoichiometric intensities. The results are shown in Fig. 3.

Typical distribution of the methane and air relative concentrations and the equivalence ratio along the jet center are shown in Fig. 3A and B for two values of the flow rates (53 cm^3/s, $Re=1645$ and 103 cm^3/s, $Re=3197$). It is clear that along the jet center, the methane concentration decreased and the air concentration increased and leveled off at above 73.5 mm above the nozzle tip. The curve representing the equivalence ratio showed that the flammable region near the jet exit was too rich in methane to ignite. The 50% ignition probability shown in Fig. 2A for the flow rate of 35 cm^3/s might be attributed to the spark size which is large enough (the long axis was 0.8–2 mm, while for the short axis it varied from about 0.4 to 1.2 mm [15]); it can expand to ignite the flammable mixture formed at the jet and air interface.

Typical distributions of the fuel and air concentrations in the radial direction are shown in Fig. 3C and D. The fuel concentration had its maximum values at the jet center and then decreased on moving into the air. The air concentration decreased to a minimum value at the jet center. The effect of the vertical location on the fuel and air distributions is shown in Fig. 3E and F, for which the jet flow rate is 70 cm^3/s ($Re=2173$). At 86 mm above the nozzle tip, the equivalence ratio remained near 1 from the jet axis out to 3 mm off the jet axis (two times the jet diameter). It then decreased to the lean side towards the air side. At 48.5 mm above the nozzle tip, the equivalence ratio decreased from about 1.6 on the jet axis to the stoichiometric value in the region 5–6 mm off the jet axis. In Fig. 4 we present the distributions of the equivalence ratio together with the ignition probability across the jet of 70 cm^3/s ($Re=2173$) at 48.5 mm above the nozzle tip. It is clear that the measured fuel and air concentration distributions are consistent with the measured ignition probabilities.

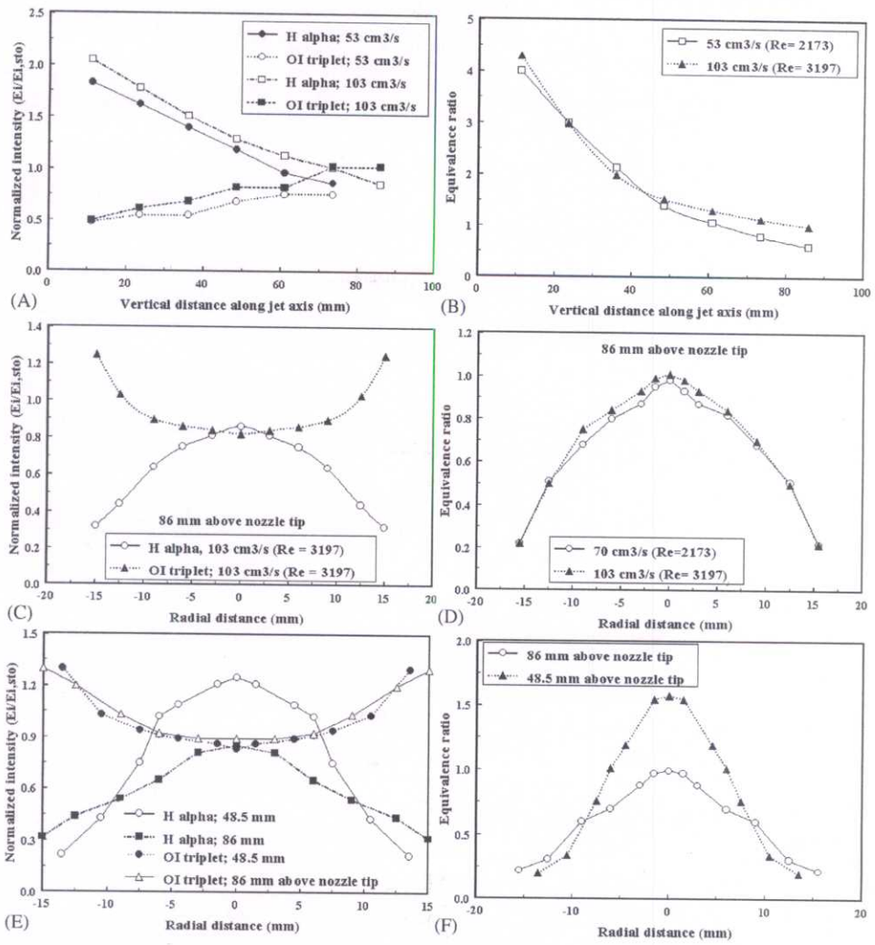

Fig. 3. Normalized emission intensities of H_α-line (656 nm) and OI triplet (777 nm) and equivalence ratio of a methane jet diffusion flame. The normalization and the equivalence ratio were estimated using the intensities measured for the stoichiometric methane–air mixture ($H_{\alpha,\,sto}$ = 185 mV; OI = 14.5 mV). A and B: in the vertical along the jet axis; C and D: in the radial direction at 86 mm above the nozzle tip; and E and F: in the radial direction, effect of the vertical locations (70 cm^3/s, Re = 2173).

3.2. Ignition and blow out times

The ignition time is defined as the time from the onset of the spark to the time when the flame was initially detectable by OH and the infrared monitors. The blow out time is defined as the time from ignition of the flame to blow out of the flame. Ignition and the development of the flame following ignition were monitored using

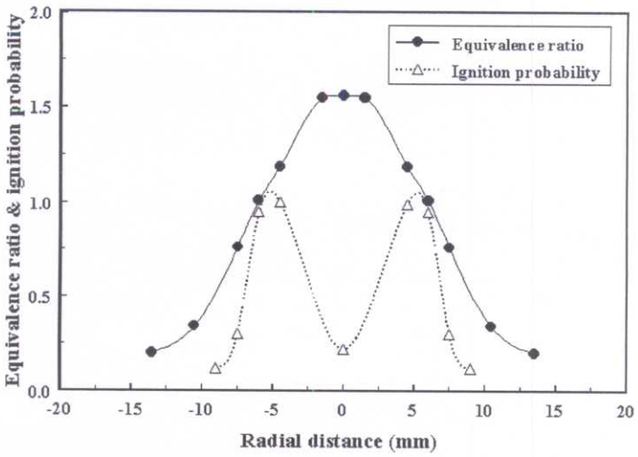

Fig. 4. Ignition probability and equivalence ratio in the radial locations for the jet flow rate of 70 cm^3/s ($Re = 2173$) at 48.5 mm above the nozzle tip.

two simple diagnostics: an unamplified photomultiplier with a 12 nm wide interference filter centered at 308 nm for detecting OH band emission and a long-wavelength visible and near-infrared photodetector. The response time of the photomultipliers is ~2 ns (<40 ns with associated cables). The response time of the photodetector was on the order of 10–100 μs. Both detectors were set up to have the field-of-view of about 60 cm in diameter which was large enough to view the entire flame under the conditions of the present experiment. Typical traces of the flame OH and infrared signals are shown in Fig. 5. It can be seen that these simple diagnostics clearly yielded information on the occurrence of the laser spark and on the starting time and the ending time of the flame. The ignition time is given by the time from the breakdown spark to initial detection of OH and the infrared signals from the flame (line A). The blow out time is given by the duration of the flame emission (line B).

Fig. 6A is a plot of the ignition times as a function of the flow rates measured for three different vertical locations. The ignition times measured along the jet axis are compared with those measured at 6 mm off the jet center in Fig. 6B. The observed ignition times range from about 4 to 10 ms. It is clear that the ignition times decreased as the vertical distance increased. For a fixed vertical location, however, variation in the ignition time with flow rate is not conclusive. For example at 73.5 and 86 mm, the ignition times decreased as the flow rates increased while at other vertical positions such as at 48.5 or 73.5 and 6 mm off the jet axis, both decreases and increases in the ignition times were observed. This variation appears to be caused by the difference in the fuel-to-air ratio at these locations. A plot of the ignition times as a function of the equivalence ratio measured at these locations shows that the ignition times correlate very well with the equivalence ratios. The ignition times are shortest in the stoichiometric region and increase towards both the rich and the lean sides. The results are shown in Fig. 7.

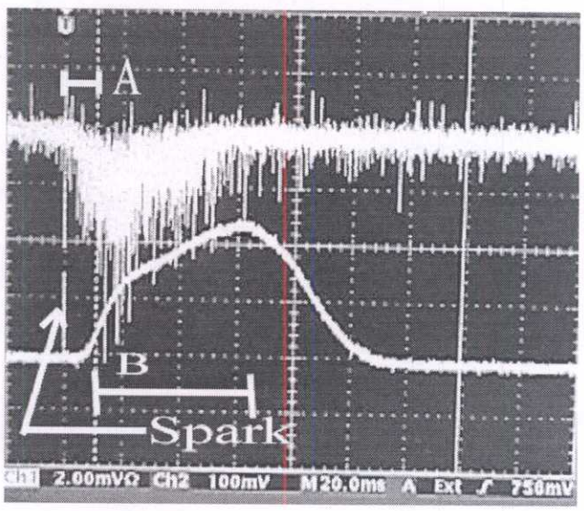

Fig. 5. Typical traces of the flame OH (upper trace) and infrared (lower) emissions for the jet flow rate of 103 cm^3/s. Line A shows the ignition time and line B shows the blow out time.

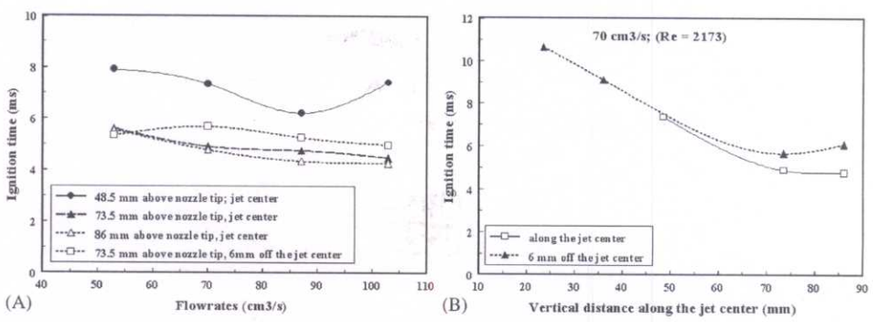

Fig. 6. Ignition time as a function of the flow rate and the vertical distance.

It must be noticed that the ignition times reported in Fig. 6 are the averaged values of over 100 experiments. In fact there are large fluctuations in the measured ignition times. This is illustrated in Fig. 8, where the ignition times measured at 86 mm above the nozzle tip for four different flow rates (53, 70, 87, and 103 cm^3/s) are presented. The ignition time varied from 3 to about 10 ms depending on the experimental conditions. For a flow rate of 53 cm^3/s, the ignition times ranging from 4.5 to about 6.7 ms were observed and about 70% of the ignition times were in the range of 4.6–6 ms. For 103 cm^3/s, the ignition times were from 4 to 4.9 ms with about 55% were around 4 ms.

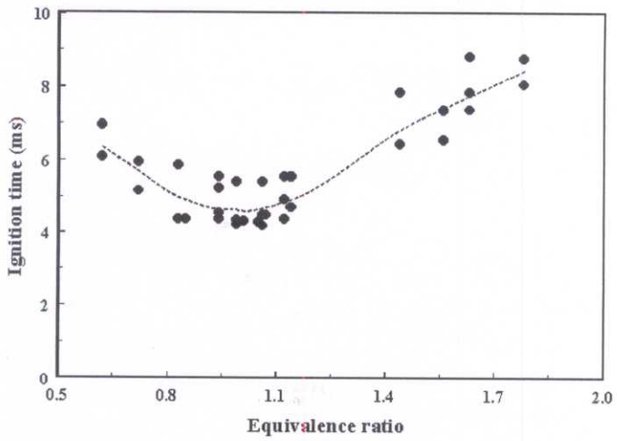

Fig. 7. Ignition time as a function of the equivalence ratio.

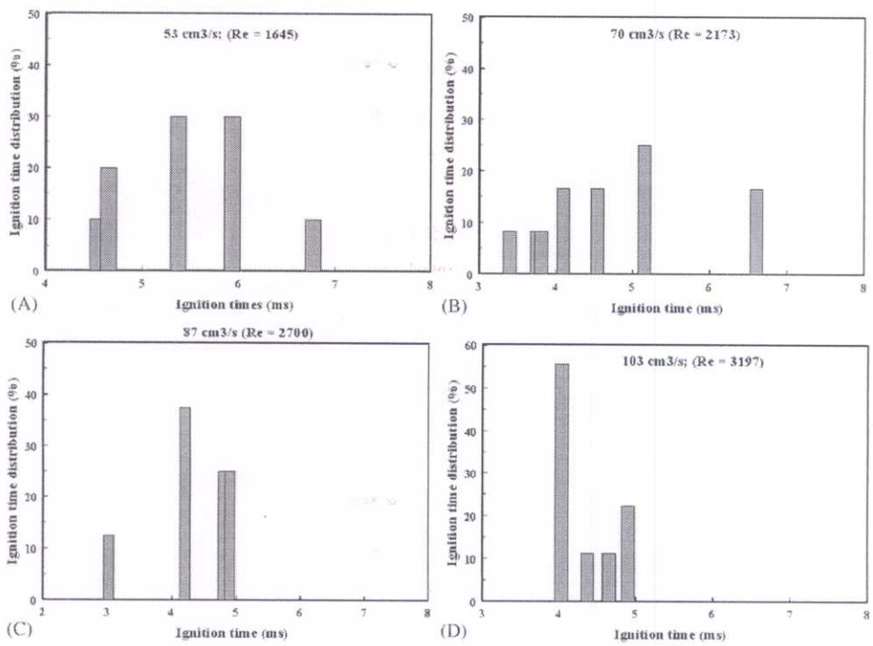

Fig. 8. Effect of the flow rates on the distribution of the ignition times for on-axis ignition at 86 mm above the nozzle tip.

Fig. 9 shows the effects of the flow rate on the blow out time when ignition was initiated on the jet axis and at 6 mm off the jet axis at 73.5 mm above the nozzle tip. Two flow rates (53 and 103 cm^3/s) were examined. At these flow rates the flame always blew out after ignition. Both the magnitude and the variability of the blow out time decreased with increasing flow rate. For the jet with a flow rate of 53 cm^3/s, when the ignition was on the jet axis, the blow out time ranged from 100 to 640 ms, but about 60% of the measured blow out times lie in the region around 200 ms. This was not the case when the ignition location was at 6 mm off the jet axis, in which case the blow out time is distributed almost evenly from 160 to 520 ms. For a flow rate of 103 cm^3/s, the blow out time varied from 60 to 100 ms with 80% of the blow out times lying within the region from 70 to 90 ms when the flame was ignited on the jet axis. When the ignition location was 6 mm off the jet axis the blow out time lie within a narrow region from 70 to about 100 ms with about 90% of the blow out times lying below 90 ms. The effect of the vertical location of the laser spark on the distribution of the blow out times is shown in Fig. 10. Here the blow out time was measured for a flow rate of 70 cm^3/s and it was ignited at 23.5 and 86 mm above the nozzle tip. It is clear that when the flame was ignited at 23.5 mm above the nozzle tip it lasts longer and the blow out times lie between 150 and 180 ms. Above this location, since only the top portion of the jet can be burnt, the blow out time became shorter. The blow out times confined tightly within 70–90 ms.

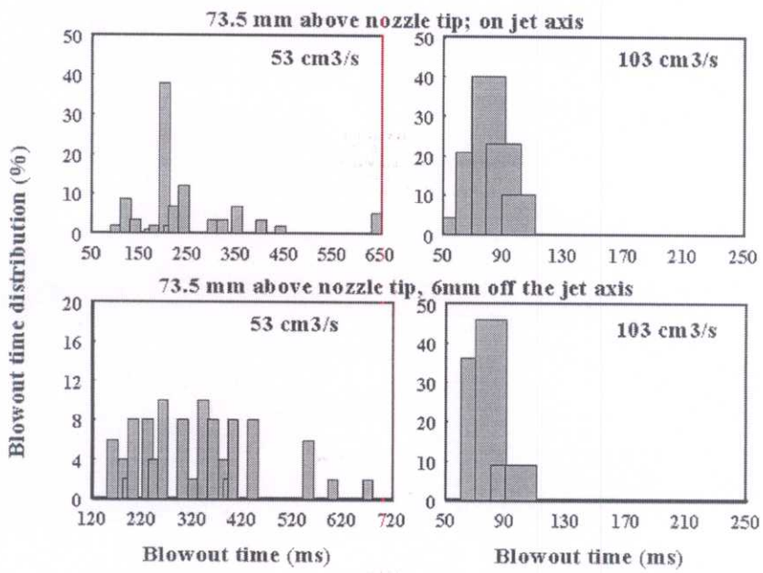

Fig. 9. Effect of the flow rates on the distribution of the blow out times for 6 mm off-axis ignition at 73.5 mm above the nozzle tip.

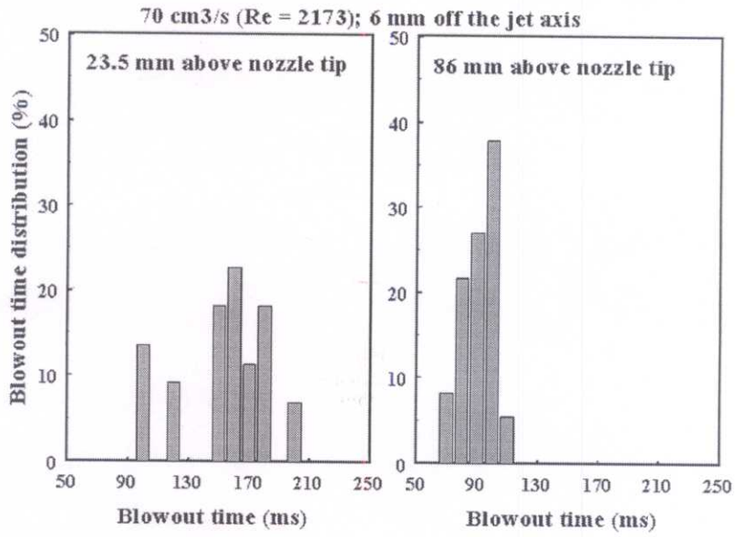

Fig. 10. Effect of the vertical distance above the nozzle tip on the distribution of the blow out times for 6 mm-axis ignition (70 cm^3/s $Re = 2173$) at 73.5 mm above the nozzle tip.

3.2.1. Ignition mechanism

It is known that when the spark is created by a laser pulse, it explodes into an expanding blast wave that propagates adiabatically until pressure equality with the surrounding gas is reached. The spark evolution usually lasts $< 100\,\mu s$ [9] which is very short (by two orders of magnitude) compared to the observed ignition times. Thus, although the shock expansion and the late-time perturbation may be important in the mixing of active reagents created by the early shock, the expanding shock could not directly ignite the jet. It then is hypothesized that after expansion the spark leaves behind a volume of very high-temperature and low-density gas. The hot ball of gas then interacts with the jet and the entrained air leading to ignition. This ignition mechanism is supported by the data on the OH emission shown in Fig. 11. Here the jet flow rate is 37 cm^3/s and the ignition location was at 23.5 mm above the nozzle tip and 6 mm off the jet axis. There are two time periods within which the OH emission was clearly detected: the early time OH emission and the late-time OH emission. In between, however, the OH emission was too weak to be detectable. The early time OH emission was due to the chemical reactions associated with the decay of the breakdown spark and the evolution of the shock. It appeared almost immediately after formation of the spark (in the order from few hundred nanoseconds to microseconds) and it disappeared after the shock expansion had stopped (about 150 μs later). The late-time OH emission was detected at about 1.5 ms after the shock expansion had ceased; its intensity continued to increase leading to ignition and full combustion of the jet. It is obvious that the late-time OH emission is due to the chemical reactions that are induced by the hot ball of gas remaining after

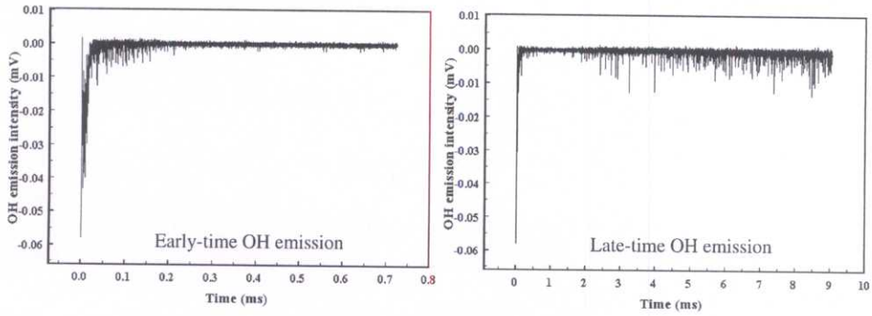

Fig. 11. Time-resolved OH emissions from an ignition event initiated at 23.5 mm above the nozzle tip, 6 mm off the jet axis, jet flow rate of 35 cm^3/s ($Re = 1086$).

the shock expansion. It is also important to report that early time OH emission was always observed in the present experiments but not all these sparks yielded successful ignition. Successful ignition, however, is always associated with a strong OH emission at later times. Thus, chemical reactions during the initial stage of the blast wave expansion are not responsible for the ignition; the ultimate fate of an ignition depends on the reactions in the later time which determines whether the gas could undergo a transition from hot plasma to a propagating flame.

4. Conclusions

We have conducted an experimental study of the laser ignition of a jet diffusion flame and shown that laser radiation can be used to effectively ignite and stabilize the flame under various turbulent flow conditions. Some preliminary results on the ignition probability, local equivalence ratio and the distribution of the ignition time and the flame blow out time are reported. The location of the optimum fuel-to-air ratio for successful ignition varies with the flow conditions. The dependence of the blow out times on the ignition locations is also presented. Off-jet axis and near-nozzle ignition locations lead to longer blow out times. These results illustrate the benefits of laser ignition for ignition and flame stabilization applications because of the ease of moving the ignition site. Data from the time-resolved OH emission from the laser spark and ignition show that possibility of the late-time chemical reactions depends on the interaction between the hot ball of gas, formed by the laser generated shock wave, and the jet and the entrained air. These interactions determine whether the gas could undergo a transition from hot plasma to a propagating flame.

References

[1] Dewhurst R. Comparative data on molecular gas breakdown thresholds in high laser-radiation fields. J Phys D 1978;11:L191–5.

[2] Rosen DI, Weyl G. Laser-induced breakdown in nitrogen and the rare gases at 0.53 and 0.35 μm. J Phys D 1987;20:1264–76.
[3] Williams W, Soileau M, Van Stryland E. Picosecond air breakdown studies at 0.53 μm. Appl Phys Lett, 1985;43:352–4.
[4] Turcu ICE, Gower MC, Huntington P. Measurement of KrF laser breakdown threshold in gases. Opt Commun 1997;134:66–8.
[5] Weyl GM. In: Radziemski LJ, Cremers DA, editors. Laser-induced plasmas and applications. New York: Marcel Dekker, 1989. p. 1–67.
[6] Phuoc TX. Laser spark ignition: experimental determination of laser-induced breakdown thresholds of combustion gases. Opt Commun 2000;175:419–23.
[7] Phuoc T, White C. Experimental studies of the absorption and emission from laser-induced spark in combustible gases. Opt Commun 2000;181:353–9.
[8] Lee J, Knystautas R. Laser spark ignition of chemically reactive gases. AIAA J 1969;7:312–7.
[9] Schmieder R. Laser spark ignition and extinction of a methane–air diffusion flame. J Appl Phys 1981;52:3000–3.
[10] Spiglanin T, MCilroy A, Fournier E, Cohen R. Time-resolved imaging of flame kernels: laser spark ignition of H_2/O_2/Ar mixtures. Combust Flame 1995;102:310–28.
[11] Syage J, Fournier E, Rianda R, Cohen R. Dynamics of flame propagation using laser-induced spark initiation: ignition energy measurements. J Appl Phys 1988;64:1499–507.
[12] Ma J, Alexander D, Poulain D. Laser spark ignition and combustion characteristics of methane–air mixtures. Combust Flame 1988;112:492–506.
[13] Lim E, McLLroy A, Ronney P, Syage J. In: Chan SH, editor. Transport phenomena in combustion. Bristol, PA: Taylor & Francis, 1996. p. 176–84.
[14] Morsy M, Ko Y, Chung S. Laser-induced ignition using a conical cavity in CH_4–air mixtures. Combust Flame 1999;119:473–82.
[15] Phuoc T, White F. Laser-induced spark ignition of CH_4/Air mixtures. Combust Flame 1999;119:203–16.
[16] Chen Y, Lewis J, Parigger C. Probability distribution of laser-induced breakdown and ignition of ammonia. J Quant Spectrosc Radiat Transfer 2000;66:41–53.
[17] Lee T, Jain V, Kozola S. Measurements of minimum Ignition energy by using laser sparks for hydrocarbon fuels in air: propane, dodecane, and jet-A fuel. Combust Flame 2001;125:1320–8.
[18] Liou LC. Laser ignition in liquid rocket engines. Proceedings of the 30th AIAA/SAE/ASME/ASEE Joint Propulsion Conference, AIAA-94-2980, Indianapolis, June 1994.
[19] Ronney P. Laser versus conventional ignition of flames. Opt Eng 1994;33:510–21.
[20] Phuoc T. Single-point versus multi-point laser ignition: experimental measurements of combustion times and pressures. Combust Flame 2000;122:508–10.
[21] Morsy M, Ko Y, Chung S, Cho P. Laser-induced two-point ignition of premixture with single-shot laser. Combust Flame 2001;125:724–7.